Tectonophysics 672–673 (2016) 24–33

Contents lists available at ScienceDirect

Tectonophysics

journal homepage: www.elsevier.com/locate/tecto

Triggered slip on a back reverse fault in the Mw6.8 2013 Lushan, China earthquake revealed by joint inversion of local strong motion accelerograms and geodetic measurements

Guohong Zhang [a,b,*], Eric A. Hetland [b], Xinjian Shan [a], Martin Vallée [c], Yunhua Liu [a], Yingfeng Zhang [a], Chunyan Qu [a]

[a] State Key Laboratory of Earthquake Dynamics, Institute of Geology, China Earthquake Administration, Beijing 100029, China
[b] Earth and Environmental Sciences, University of Michigan, Ann Arbor, USA
[c] Institut de Physique du Globe de Paris, Sorbonne Paris Cité, Université Paris Diderot, UMR 7154 CNRS, Paris, France

ARTICLE INFO

Article history:
Received 4 June 2015
Received in revised form 11 January 2016
Accepted 13 January 2016
Available online 6 February 2016

Keywords:
Triggered fault slip
Back reverse fault
Joint inversion
Local strong motion data
Geodetic measurements
The 2013 Lushan earthquake

ABSTRACT

The 2013 Mw6.8 Lushan, China earthquake occurred in the southwestern end of the Longmenshan fault zone. We jointly invert local strong motion data and geodetic measurements of coseismic surface deformation, including GPS and InSAR, to obtain a robust model of the rupture process of the 2013 Lushan earthquake. Our joint inversion best model involves the rupture of two opposing faults during the Lushan earthquake, a main fault and a secondary fault. It is only when the secondary fault is included that both the GPS and InSAR measurements are fit along with the near-field strong motion. Over 75% of the computed moment was released in slip on the main fault segment, a northwest dipping, listric thrust fault, with buried thrust and dextral strike-slip at hypocenter depths, and with only minor slip closer to the surface. The secondary fault mainly involved oblique thrust slip or pure dextral strike-slip at shallower depths, and accounts for just under 24% of the moment released in the Lushan earthquake. Coulomb stress changes of about 0.5 MPa on the secondary fault segment at the time coseismic slip initiated on that fault indicate that slip was likely triggered by the coseismic slip on the main blind thrust fault. Our coseismic slip model is consistent with a sub-horizontal and east–west to southeast–northwest trending most compressive stress. Our inferred coseismic slip model is also consistent with previous GPS derived models of strain accumulation on the Longmenshan fault system.

1. Introduction

The magnitude 6.8 Lushan earthquake occurred on April 20, 2013 in Sichuan province, China, and resulted in 198 casualties, tens of thousands of injuries, and damages totaling 6.8 billion USD (EM-DAT). The epicenter of the Lushan earthquake is located at (30.291°N, 102.983°E) and the hypocentral depth is 17.6 km (Fang et al., 2013). The Lushan region is in the southwestern part of the Longmenshan fault zone (LMSF), which also hosted the 2008 Mw7.9 Wenchuan earthquake to the northeast. The LMSF is the margin between the Tibetan plateau and the Sichuan Basin, and is a northeast–southwest striking and northwest dipping fault zone (Burchfiel, 2008; Fig. 1a). The LMSF had been widely considered to be of low earthquake risk before the 2008 Wenchuan earthquake, due to the low level of seismicity on the LMSF and the slow moment accumulation rate inferred from geodetic observations (Zhang, 2013), although including non-elastic effects in the earthquake cycle model may reconcile the low GPS rates with a short recurrence time of large earthquakes (Thompson et al., 2015). The Lushan earthquake occurred roughly 90 km to the southwest of the 2008 Wenchuan earthquake (Fig. 1). Parsons et al. (2008) inferred only a slight positive coulomb stress change (CSC) contribution from the Wenchuan earthquake in the region of the Lushan earthquake. To date, there have been no other significant earthquakes on the LMSF (Zhang et al., 2010), and the region between the Lushan and Wenchuan earthquakes likely poses a significant ongoing earthquake risk (e.g., Shan et al., 2013).

The Lushan earthquake occurred in a complex tectonic region, just to the north of an area that can be loosely referred to as a triple junction, with the Sichuan Basin to the east and the Songpan and Dianzhong blocks to the northwest and south, respectively (Fig. 1a). The LMSF is the boundary between the Songpan block and the Sichuan Basin, and the Songpan block is bounded by the Xianshuihe fault (XSHF) on the west. To the south, the Anninghe fault (ANHF) separates the Dianzhong block from the Sichuan Basin (Fig. 1). Both the XSHF and ANHF are large active strike-slip faults, with a dextral strike-slip rate of > 10 mm/yr and 3–8 mm/yr, respectively (e.g., King et al., 1997; Wang et al., 2008). In contrast, the LMSF has components of both thrust and dextral strike-slip motion, which was revealed by GPS observations prior to the 2008 Wenchuan earthquake (e.g., Shen et al., 2005; Meade, 2007), as

* Corresponding author at: Hua Yan Li Jia Yi Hao, Chaoyang district, Beijing 100029, China.
E-mail address: zhanggh@ies.ac.cn (G. Zhang).

http://dx.doi.org/10.1016/j.tecto.2016.01.031
0040-1951/

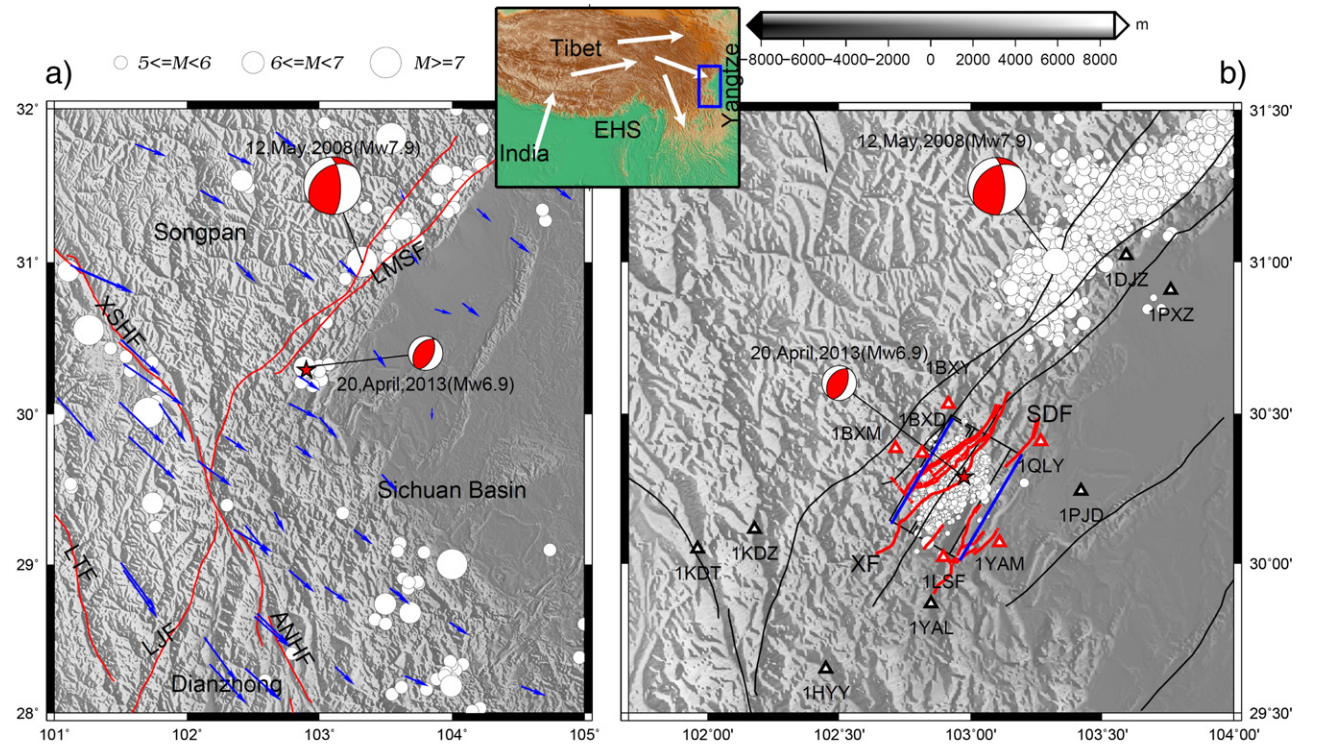

Fig. 1. Tectonic setting of the 2013 Lushan earthquake, with locations of the strong motion stations (red triangles), mapped faults (solid lines), epicenters of earthquakes Ms > 5.0 between 1901 and 2014 from Global CMT (which circles, symbol size scales with magnitude), and epicenter of the 2013 Lushan earthquake (red star). (a) The two focal mechanisms are the 2008 Wenchuan and the 2013 Lushan earthquakes. GPS measured crustal motion by Gan et al. (2007) is shown as blue vectors. (b) Thick red lines and triangles are local faults and stations, respectively. Triangles with thick red outlines are stations displayed in Fig. 4, which are used to demonstrate the differences between the optimal inversion with the segment F4 and the inversion test without it. Black outlines are stations not used for comparison between the optimal inversion and the inversion test. Blue lines are intersections of the fault model projected to the surface. Acronyms: EHS, Eastern Himalaya Syntaxis; YZ, Yangtze; XSHF, Xianshuihe fault; LMSF, Longmenshan fault; LJF, Lijiang–Xiaojinhe fault; ANHF, Anninghe fault; XJF, (Zemuhe–)Xiaojiang fault; LTF, Litang fault; XF: Xinkaidian fault; SDF: Shuangshi–Dachuan fault.

well as coseismic slip models of that earthquake (e.g., Medina Luna and Hetland, 2013; Styron and Hetland, 2015).

Field investigations conducted after the Lushan earthquake, focal mechanisms of the earthquake, and distribution of aftershocks all suggest that there is a degree of complexity in the geometry of the faults that ruptured in the Lushan earthquake (Li et al., 2013; Xu et al., 2013; Fang et al., 2013). Li et al. (2013) argued that the local geologic setting of the 2013 Lushan region is very complicated, consisting of both northeast striking faults, consistent with the overall trend of the LMSF, and northwest striking transform faults. They also pointed out that the Lushan event initiated on a detachment underneath the frontal Longmenshan range between the Shuangshi–Dachuan fault (SDF) and the Xinkaidian fault (XF) based on observations of surface cracks indicative of slip on a shallow dipping fault at depth (Li et al., 2013). Li et al. (2014) further argued that the Lushan earthquake occurred on a portion of a blind thrust at the front of the Longmenshan range, which is linked to a detachment that extends into the Sichuan basin. Focal mechanisms determined for the Lushan earthquake by Global CMT and USGS W-phase CMT indicated that the coseismic slip was thrust; however, several of the focal mechanisms contained non-double-couple components, which might either be due to poor resolution of the inferred focal mechanism or may also indicate a variation in fault geometry or rake in the Lushan earthquake. Finally, relocated aftershocks reveal a cluster of events extending into the hanging wall of the thrust fault that likely ruptured in the Lushan earthquake (Fang et al., 2013; Fig. 2a). The larger Wenchuan earthquake that occurred to the northeast on the LMSF was characterized by fairly complicated coseismic slip, with large rake variations on variably dipping faults (e.g., Shen et al., 2009; Feng et al., 2010; Zhang et al., 2011; Wang et al., 2011). Given the complexity of slip in the earlier Wenchuan earthquake, it might follow that the Lushan earthquake might also be characterized by complexities in slip, albeit to a lesser degree and with more compact slip than in the Wenchuan earthquake, due to the fact that the 2013 Lushan event has much smaller magnitude. Additionally, since the 2008 Wenchuan event obliquely ruptured an unusually highly dipping (~50° in the shallow portions of the fault), listric fault (Zhang et al., 2010), it is natural to ask whether the Lushan event also involved slip on a low-angle detachment at depth or if it was entirely constrained on a high-angle thrust fault.

There have been several published coseismic slip models of the Lushan earthquake. Hao et al. (2013) and Zhang et al. (2014) both used local strong motion and teleseismic data and inferred similar slip distribution models, demonstrating predominantly thrust motion on a relatively high-angle blind fault. Jiang et al. (2014) derived a fault slip model based on local GPS data, and indicated that the GPS data required significant sinistral strike-slip in addition to the dominant thrust slip. Note that these previous studies all assumed single, planar fault geometries, and used either the seismic or geodetic data separately. As the regional tectonic setting is somewhat complex, the assumption that only a single planar fault slipped in the Lushan earthquake may not be complete. Moreover, using both seismic and geodetic data it may be possible to better constrain the fault geometry and rupture process (see Supplementary material).

In this study, we infer the fault geometry and spatio-temporal evolution of the rupture process in the 2013 Lushan earthquake using a joint inversion of local strong motion, GPS, and InSAR data. The strong motion stations we use are all relatively close to the source area (Fig. 1b), and the data from them provides valuable constraints on the spatiotemporal coseismic slip distribution (see Supplementary material), allowing us to determine whether there are some delayed or triggered slip in the